

1 **African origin haplotype protective for Alzheimer's disease in *APOE*ε4 carriers: exploring**  
2 **potential mechanisms**

3 **Authors**

4 Luciana Bertholim-Nasciben<sup>1</sup>, Karen Nuytemans<sup>1,2</sup>, Derek Van Booven<sup>1</sup>, Farid Rajabli<sup>1,2</sup>, Sofia Moura<sup>1</sup>,  
5 Aura M. Ramirez<sup>1</sup>, Derek M. Dykxhoorn<sup>1,2</sup>, Liyong Wang<sup>1,2</sup>, William K. Scott<sup>1,2</sup>, David A. Davis<sup>3</sup>, Regina T.  
6 Vontell<sup>3</sup>, Katalina F. McInerney<sup>4</sup>, Michael L. Cuccaro<sup>1,2</sup>, Goldie S. Byrd<sup>5</sup>, Jonathan L. Haines<sup>6</sup>, Marla  
7 Gearing<sup>7</sup>, Larry D. Adams<sup>1</sup>, Margaret A. Pericak-Vance<sup>1,2</sup>, ADSP<sup>8</sup>, Juan I. Young<sup>1,2</sup>, Anthony J.  
8 Griswold<sup>1,2,\*,#</sup>, and Jeffery M. Vance<sup>1,2,\*,#</sup>

9 (1) John P. Hussman Institute for Human Genomics, University of Miami Miller School of Medicine, Miami, FL, USA (2) Dr. John T.  
10 Macdonald Foundation Department of Human Genetics, University of Miami Miller School of Medicine, Miami, FL, USA (3) Brain  
11 Endowment Bank, Department of Neurology, University of Miami Miller School of Medicine, Miami, FL, USA (4) Department of  
12 Neurology, Miller School of Medicine, Miami, FL, USA (5) Maya Angelou Center for Health Equity, Wake Forest University, Winston-  
13 Salem, NC, USA (6) Cleveland Institute for Computational Biology, Case Western Reserve University, Cleveland, Ohio, USA (7)  
14 Goizueta Alzheimer's Disease Research Center, Emory University, Atlanta, GA, USA (8) Alzheimer's Disease Sequencing Project

15 #These authors contributed equally

16 \*Correspondence: [agriswold@med.miami.edu](mailto:agriswold@med.miami.edu) (A.J.G.), [jvance@med.miami.edu](mailto:jvance@med.miami.edu) (J.M.V.)

17 **Abstract**

18 *APOE*ε4 is the strongest genetic risk factor for Alzheimer's disease (AD) with  
19 approximately 50% of AD patients carrying at least one *APOE*ε4 allele. Our group identified a  
20 protective interaction between *APOE*ε4 with the African-specific A allele of rs10423769, which  
21 reduces the AD risk effect of *APOE*ε4 homozygotes by approximately 75%. The protective variant  
22 lies 2Mb from *APOE* in a region of segmental duplications (SD) of chromosome 19 containing a  
23 cluster of pregnancy specific beta-1 glycoprotein genes (*PSGs*) and a long non-coding RNA.  
24 Using both short and long read sequencing, we demonstrate that rs10423769\_A allele lies within  
25 a unique single haplotype inside this region of segmental duplication. We identified the protective  
26 haplotype in all African ancestry populations studied, including both West and East Africans,  
27 suggesting the variant has an old origin. Long-read sequencing identified both structural and DNA

28 methylation differences between the protective rs10423769\_A allele and non-protective  
29 haplotypes. An expanded variable number tandem repeat (VNTR) containing multiple MEF2  
30 family transcription factor binding motifs was found associated with the protective haplotype ( $p$ -  
31 value =  $2.9e-10$ ). These findings provide novel insights into the mechanisms of this African-origin  
32 protective variant for AD in *APOE* $\epsilon$ 4 carriers and supports the importance of including all  
33 ancestries in AD research.

## 34 Introduction

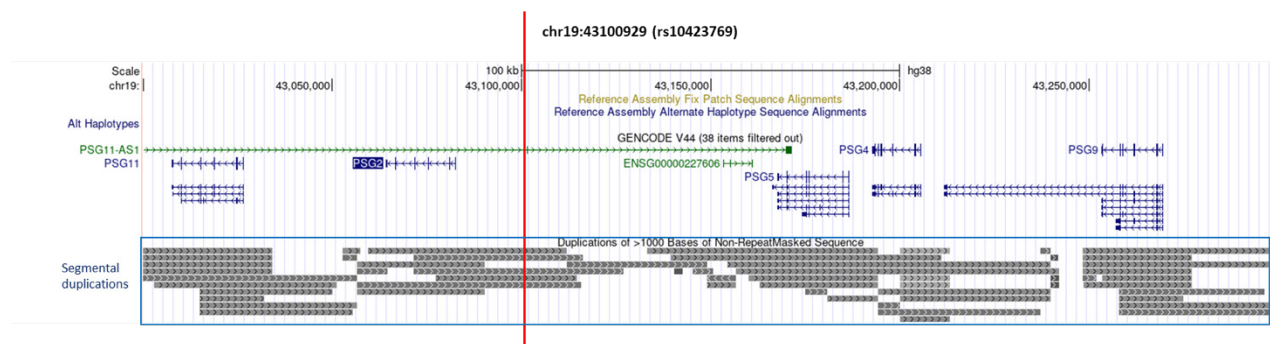
35 Individuals with local African (AFR) ancestral genetic background surrounding *APOE* $\epsilon$ 4  
36 have decreased AD risk associated with the *APOE* $\epsilon$ 4 allele compared to individuals of European  
37 ancestry, thereby demonstrating some natural protective effect in the AFR background.<sup>1,2</sup> We  
38 recently identified a strong protective interaction between *APOE* $\epsilon$ 4 and the A allele of rs10423769,  
39 which reduces the AD risk effect of *APOE* $\epsilon$ 4 homozygotes by approximately 75% in African  
40 Americans (AA), AFR individuals from Ibadan (Nigeria), and genetically admixed Puerto Rican  
41 individuals.<sup>3</sup> The frequency of the minor rs10423769 A allele is ~12% in AFR but only ~0.03% in  
42 EUR populations. This protective locus is located 2Mb upstream of *APOE* and lies within a highly  
43 segmentally duplicated region of chr19 containing a cluster of pregnancy-specific  $\beta$ -1 glycoprotein  
44 (*PSG*) genes as well a long non-coding RNA (ENSG00000282943) (Figure 1). Interestingly, the  
45 *PSG* genes are primarily expressed in the placenta with little, if any, expression in the brain.<sup>4,5</sup>

46 The mechanisms involved in the protective interaction of this locus with *APOE* $\epsilon$ 4 are  
47 unknown. However, molecular investigation of the protective locus is complicated by its genomic  
48 context. The *PSG* region is rich in segmental duplications (SDs) that are difficult to resolve using  
49 short-read sequencing data, as traditional sequencing reads are not long enough to be precisely  
50 aligned to a specific locus in these repetitive regions.<sup>6</sup> In addition, SDs constitute hotspots of  
51 recurrent rearrangement by nonallelic homologous recombination, resulting in high occurrence of  
52 copy number variations (CNVs), gene conversion, and structural variants (SVs)<sup>7,8</sup>. SVs could

53 affect chromatin structure, which we have previously described as differing between AFR and  
54 EUR brain astrocytes.<sup>9,10</sup> In addition, the SD region of the *PSGs* has been previously reported to  
55 have many deletions and duplications that vary between ancestries.<sup>4</sup>

56 To gain insight into its mechanisms of protection, we performed an initial genetic  
57 characterization of this protective locus. First, we refined the haplotype harboring the protective  
58 locus using a large, short read-sequencing database, including individuals from diverse ancestries  
59 from the Alzheimer's Disease Sequencing Project (ADSP). Second, we used long-read  
60 sequencing to confirm the location of the haplotype in this highly segmentally duplicated region  
61 of chromosome 19. Third, we used the long-read sequencing data to identify the SVs and DNA  
62 methylation profiles in the *PSG* region. Finally, we explored an expanded variable number tandem  
63 repeat (VNTR) enriched in multiple MEF2 family transcription factors binding motifs present in this  
64 genomic region. These findings provide novel insights into the potential mechanisms underlying  
65 this AFR-origin protective variant for AD in *APOE* $\epsilon$ 4 carriers. Although biologically complex, a  
66 better understanding of the genetic and molecular factors involved in the protection against risk  
67 of *APOE* $\epsilon$ 4 driven by this region presents a therapeutic opportunity for all ancestries.

68



69

70 Figure 1. UCSC browser view of surrounding region of rs10423769\_A allele (marked by vertical red line). The annotation of segmental  
71 duplication includes all non-allelic intrachromosomal and interchromosomal alignments greater than 1 kb and with more than 90% of  
72 sequence identity, excluding common repeats or satellite sequences.

73

## 74 **Methods**

### 75 **Haplotype block analysis**

76 We extracted phased genotype data from rs10423769\_A allele carriers from the  
77 Alzheimer's Disease Sequencing Project Release 4 (ADSP R4: ng00067.v10) of short-read whole  
78 genome sequencing ([Web resources](#)). In the region of 70 kb surrounding rs10423769, we  
79 selected all SNPs with a MAF  $\geq$  0.05 and Hardy–Weinberg equilibrium (HWE) exact test p-value  
80  $>$  0.001 in the African population of the 1000 Genomes project (1000G) dataset for analysis  
81 (n=301).<sup>11</sup> Haploview 4.2 software was used to define the haplotype blocks.<sup>12</sup> Plink v1.90<sup>13</sup> ([Web  
82 resources](#)) was used to calculate Linkage Disequilibrium (LD) using ADSP R4. LDhap from the  
83 LDlink (5.6.5 Release) web-based application<sup>14</sup> ([Web resources](#)) was used to map and calculate  
84 frequencies of the haplotypes harboring the rs10423769\_A allele across population groups from  
85 the 1000G Phase 3.

### 86 **Long read whole genome sequencing (LRWGS)**

87 LRWGS was generated from DNA extracted from either cerebellum samples excised from  
88 frozen brain or peripheral blood samples from 38 individuals that were heterozygous or  
89 homozygous for rs10423769\_A, or non-carriers, as described in Supplementary Table 1. Brain  
90 samples were obtained from the biorepository of the John P. Hussman Institute for Human  
91 Genomics (HIHG) and Brain Endowment Bank at the University of Miami, as well as Emory  
92 University Goizueta Alzheimer's Disease Research Center (GADRC) Brain Bank. Blood samples  
93 were obtained from participants as part of ongoing research projects in studying Alzheimer's  
94 disease in individuals of African ancestries (AG052410 and AG072547, P.I. M. Pericak-Vance).

95 DNA was extracted in the HIHG biorepository using the AutoGen FlexSTAR using  
96 standard procedures without further size selection. Libraries were constructed using the SQK-  
97 LSK109 ligation kit from Oxford Nanopore Technology (ONT). Samples were loaded onto

98 PromethION R9.4.1 flow cells and sequenced in 72-hour data acquisition runs on the  
99 PromethION24 device. Base calling was performed with Guppy version 3.3.2 which  
100 simultaneously produces MM and ML methylation tags in the unaligned bam file. Resulting bam  
101 files were then converted to fastq files (samtools v1.2) preserving these tags in the meta data for  
102 each read). Resulting FASTQs were aligned to GRCh38 using minimap2 v2.17-r941 where the  
103 methylation tags were preserved from the previous step. Small variant calling was performed with  
104 Clair3 (v1.0.3). Sniffles2 (v2.0.7) was used for structural variant calling (default parameters were  
105 used individually on each sample, then a joint call was performed with default parameters with  
106 sniffles2). Aligned BAM files were examined using the Integrative Genome Viewer v.2.4.10 ([Web  
107 resources](#)) in Third Gen quick consensus mode.

#### 108 **Local assembly and motif finding**

109 TREAT (Tandem REpeat Annotation Toolkit) assembly tool with Otter <sup>15</sup> ([Web resources](#))  
110 was used for local assembly of tandem repeat regions in chr19 and annotation of VNTRs. The  
111 association between rs10423769 allele and the tandem repeat region length measured in bp was  
112 evaluated using Wilcoxon rank sum test. MEME Suite <sup>16</sup> ([Web resources](#)) was used for de novo  
113 motif finding and the algorithm FIMO (version 5.5.5) <sup>17</sup> within MEME Suite was used to identify  
114 known transcription factors (TF) binding motifs in the region. We screened defined transcription  
115 factors binding site databases JASPAR CORE 2022 (vertebrates non-redundant) <sup>18</sup> and selected  
116 those binding sites with q-value < 0.001.

#### 117 **Allele-specific differential methylation analysis**

118 BAM files with methylation tags were phased by Longshot v0.4.5 <sup>19</sup> using a region of +/-  
119 40 kb from rs10423769 with a minimum coverage of 10 and minimum alternative allele fraction of  
120 0.35. Allele-specific bedmethyl files with aggregation of modified bases were obtained with the  
121 tool modkit v0.1.12 ([Web resources](#)) with the options --partition-tag HP, --combine-strands, --cpg,

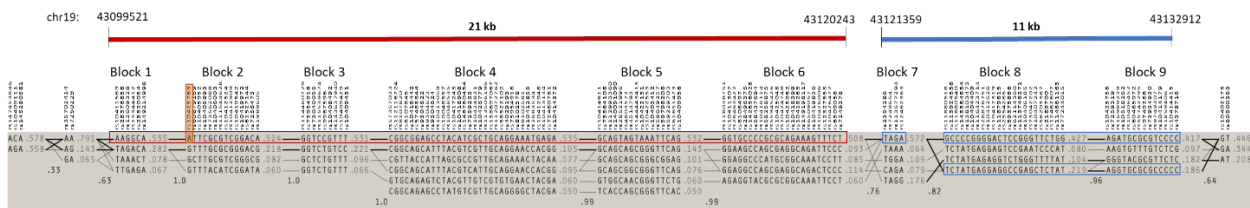
122 and --ignore h. The DMA module from Nanomethphase v 1.2.0 <sup>20</sup> were used for differential  
123 methylation analysis with -smf set to FALSE.

## 124 Results

### 125 Haplotype block analysis (based on short-read ADSP data)

126 We determined the composition of the haplotype harboring the rs10423769\_A using the  
127 ADSP R4 set of short read whole genome sequencing. We identified 1,962 individuals carrying  
128 at least one rs10423769\_A allele. Six haplotype blocks were identified in the region surrounding  
129 rs10423769\_A (Figure 2). No recombination is observed between the most frequent haplotypes  
130 (~53%) in block 1, block 2 (harboring the rs10423769\_A) and the remaining blocks 3-6.  
131 Supporting this, rs10423769 has a  $D' > 0.95$  ( $LOD \geq 2$ ) with all SNPs from these six blocks, with  
132 the exception of two positions (rs8107144 and rs7250796) with  $D' < 0.3$ . Thus, we determined  
133 that the minimum shared haplotype harboring rs10423769\_A allele was approximately 21kb  
134 (chr19:43099521-43120243) spanning six haplotype blocks. An extended haplotype including  
135 blocks 7-9 (chr19:43121359- 43132912) was also identified with a  $D' = 0.76$  between blocks 6  
136 and 7.

137



139

140 **Figure 2.** Haplotype blocks identified in 1,962 individuals carrying at least one rs10423769\_A allele using Haploview 4.2 and ADSP.  
141 Lines between blocks indicate co-occurrence of adjacent haplotypes in individuals with line thickness representing frequency of co-  
142 occurrence across individuals. Haplotype block frequencies are shown in the right of each block ( $\geq 0.05$ ). Multi-allelic  $D'$  is shown on  
143 the bottom of crossing areas, which represents the level of recombination between blocks. Blocks with  $D' > 0.8$  were considered the

144 same haplotype. Rs10423769 is marked by an orange box. The 21kb (chr19:43099521-43120243) minimum shared haplotype is  
145 marked by a red box and the 11 kb extended haplotype (chr19:43121359- 43132912) is marked by blue boxes.

146 In order to support these findings, we performed LD analysis using  $r^2$  statistics and the  
147 entire ADSP R4 dataset of ~36,000 individuals, which showed almost perfect linkage ( $r^2 > 0.95$ )  
148 between rs10423769\_A and 13 markers distributed along the six blocks of the 21 kb minimum  
149 shared haplotype (Supplementary Table 2). Eleven markers distributed along the 11 kb extended  
150 haplotype showed  $r^2 > 0.75$ .

### 151 Frequency of the haplotype across populations

152 Using the allele frequency information from 1000G to verify the population-specific  
153 frequency of the 21 kb minimum shared haplotype, we found the same haplotype across multiple  
154 admixed populations containing African ancestry (African American, Afro-Caribbean, and Puerto  
155 Ricans admixed populations) (Figure 3), but not in individuals of Mexican, Peruvian, East Asian,  
156 South Asian or European populations. Interestingly, the haplotype frequency was similar between  
157 West (Nigeria) and East (Kenya) populations.

158

| Rs number   | Allele |
|-------------|--------|
| rs10411569  | A      |
| rs13344412  | G      |
| rs10423769  | A      |
| rs10405993  | C      |
| rs1989605   | A      |
| rs9967596   | C      |
| rs10416442  | G      |
| rs9304622   | A      |
| rs9304624   | C      |
| rs10413059  | C      |
| rs10418908  | A      |
| rs10424831  | G      |
| rs10426779  | C      |
| rs10412855  | A      |
| rs10412948  | G      |
| rs10413134  | A      |
| rs28521996  | T      |
| rs144443413 | T      |
| rs10422131  | A      |
| rs10422553  | A      |
| rs10402412  | A      |
| rs28463422  | T      |
| rs28496375  | C      |
| rs10418114  | C      |
| rs10425962  | A      |
| rs10418263  | A      |
| rs10426472  | T      |

| Population                       | Frequency |
|----------------------------------|-----------|
| Yoruba, Nigeria [YRI]            | 0.11      |
| Luhya, Kenya [LWK]               | 0.14      |
| Gambian, Gambia [GWD]            | 0.12      |
| Mende, Sierra Leone [MSL]        | 0.11      |
| Esan, Nigeria [ESN]              | 0.09      |
| African Americans, USA [ASW]     | 0.11      |
| Afro-Caribbean, Barbados [ACB]   | 0.09      |
| Puerto Ricans, Puerto Rico [PUR] | 0.02      |

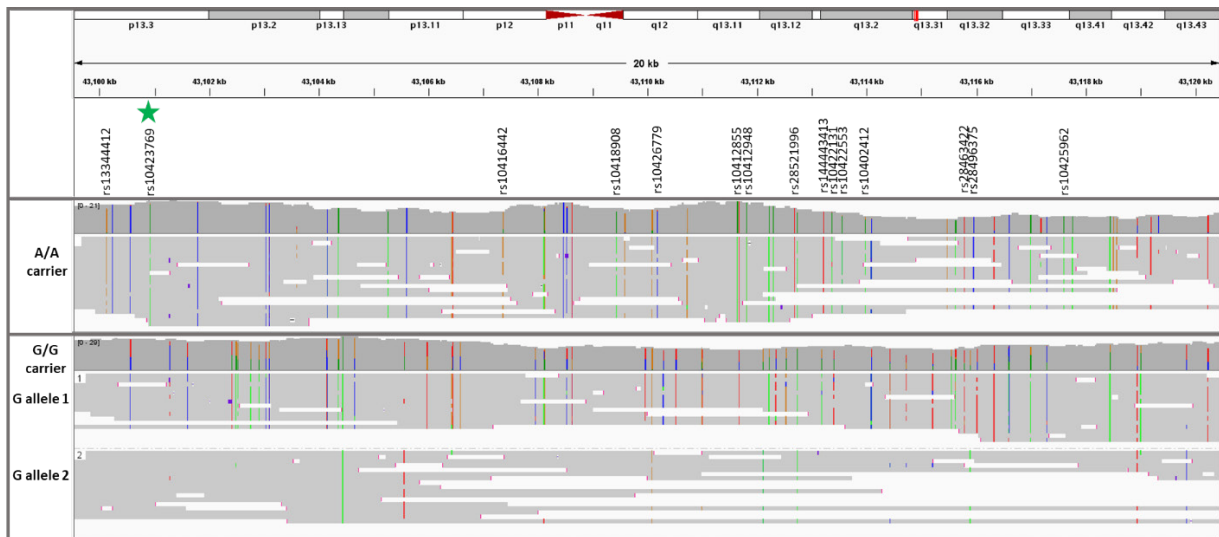
159

160 **Figure 3.** Population-specific frequency of the minimum shared haplotype harboring the rs10423769\_A allele in 1000G. LD pruned  
161 haplotype across 10 blocks determined by Haploview are shown. Frequencies were calculated with the tool LDhap from LDlink web-  
162 based application.

163

### 164 Validation of minimum shared haplotype with LRWGS

165 Since rs10423769\_A allele is in an area of segmental duplication, LRWGS was used to  
166 validate whether rs10423769 is a true variant or an artifact of incorrect mapping in the SD region.  
167 LRWGS of 38 brain and blood samples including rs10423769\_A homozygous, heterozygous and  
168 non-carriers (Supplementary Table 1) was performed with ONT yielding an average genome  
169 coverage of  $21.5 \pm 5.3X$  and average read length of  $10.4 \pm 3.0$  kb. The average depth of high-  
170 quality reads ( $MAPQ \geq 60$ ) for the rs10423769\_A position (chr19:43100929) was  $16.0 \pm 4.9X$  and  
171 all reads mapped uniquely for this specific position. In addition, analysis of potential secondary  
172 alignments of reads spanning the 21 kb minimum shared haplotype confirmed that the variant  
173 pattern identified along the haplotype block are specific to this region and not found contiguously  
174 in any other region of the genome (Figure 4). The frequency of variants in almost perfect linkage  
175 disequilibrium ( $r^2 > 0.95$ ) were confirmed in the LRWGS variant calling (Supplementary Table 2).



176



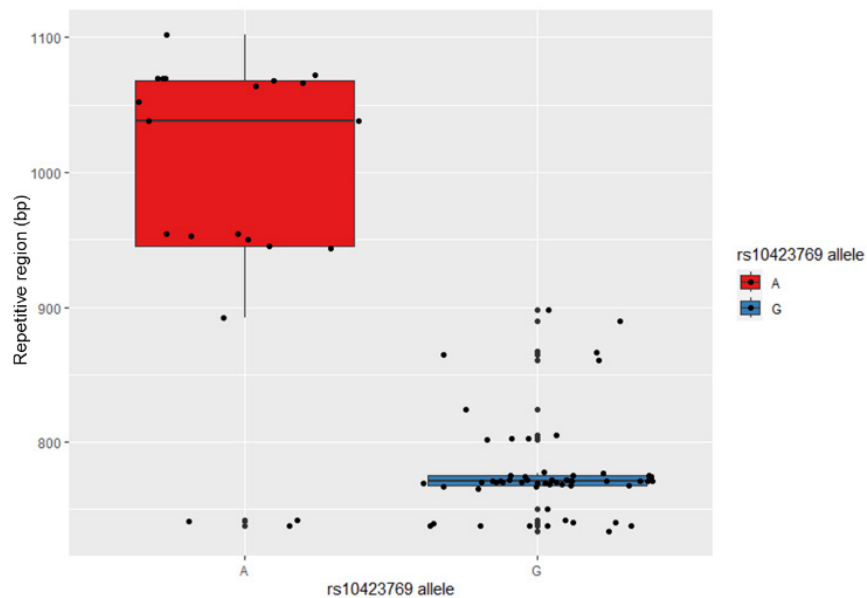
177 **Figure 4.** Read the coverage and map of the 21 kb minimum shared haplotype from two representative individuals homozygous for  
178 either the rs10423769\_A or rs10423769\_G alleles. The green star marker represents the rs10423769\_A allele, and all other listed  
179 markers are in LD>0.95 with rs10423769\_A. Colored lines represent IGV consensus SNPs: A, green; C, blue; T, red; G, orange.

180

## 181 **Analysis of structural variation**

182 After mapping the haplotype associated with rs10423769\_A, we explored other genomic  
183 and epigenomic features that could contribute to the functional mechanisms involved in the  
184 protection afforded by this locus. The LRWGS data were used to detect germline SVs in the 2 Mb  
185 region (chr19: 43000000-45000000) spanning from the protective locus to *APOE*. Sniffles2  
186 identified 87 SVs in the region, including 42 deletions, 43 insertions, and two breakends. One  
187 insertion located at chr19:43132126 (32 kb from rs10423769) was identified with a frequency of  
188 0.80 in rs10423769\_A homozygotes and 0.07 in non-carriers. This insertion is located in an  
189 annotated repetitive region (772bp, chr19:43,131,850-43,132,621) ([Web resources](#))  
190 approximately 32 kb from the protective locus, on block 9 of the expanded haplotype (Figure 2).  
191 Further investigation of the 772bp region of the reference genome indicates the presence of a  
192 VNTR with repetitions of a 29 bp tandem repeat pattern. Local assembly of this region revealed  
193 that the A allele is associated with expanded VNTR alleles (p-value = 2.944e-10, Figure 5)  
194 containing a higher number of the 29 bp tandem repeat. We analyzed the region for the presence  
195 of motifs and known TF binding sites and identified that the 29 bp repetitive sequence carries  
196 predicted binding sites motifs for the MEF2 family of transcription factors. MEF2D had the highest  
197 score by FIMO motif finding tool, <sup>17,18</sup> followed by MEF2B and MEF2A (Figure 6).

198



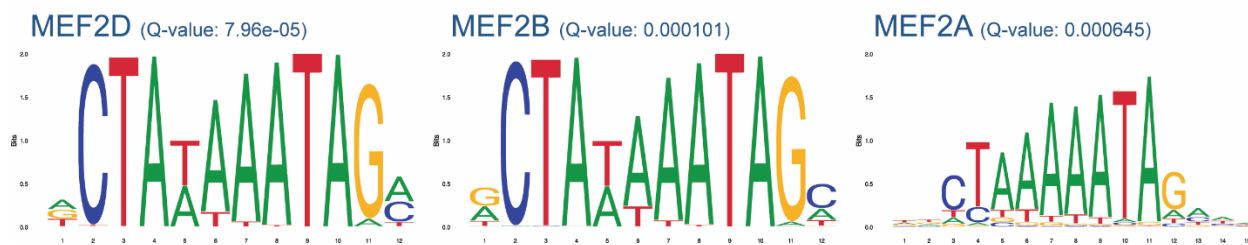
199

200 **Figure 5.** VNTR length correlation with rs10423769 haplotype (p-value = 2.944e-10).

**A**



**B**



201

202 **Figure 6.** Motif analysis of the expanded VNTR allele associated with rs10423769\_A. **A.** 29 bp Repetitive sequence identified by  
203 MEME Suite <sup>16</sup>. **B.** MEF2 family of TF binding motifs with FIMO motif finding tool q-value <sup>17,18</sup>.

204

## 205 Differential methylation analysis

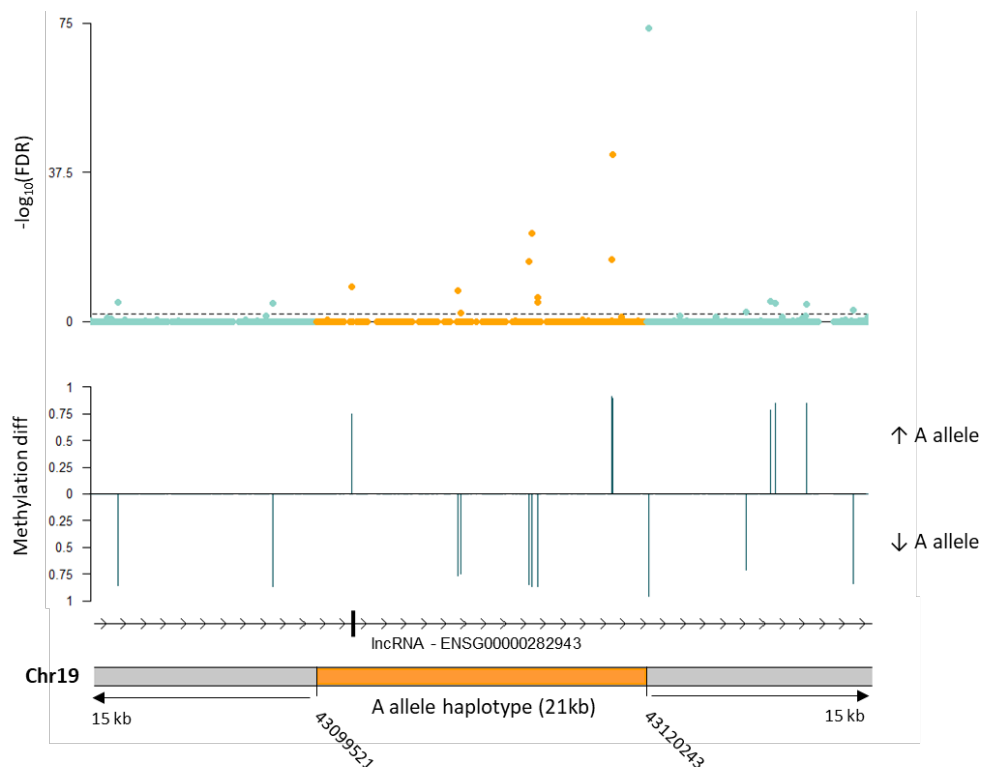
206

207

208

We also hypothesized that the mechanism of protection could be related to differential DNA methylation at the haplotype. Thus, we performed allele-specific methylation analysis of five heterozygote rs10423769\_A/G brain samples to evaluate methylation differences in the 21 kb

209 minimum shared haplotype and surrounding region. We identified 17 differentially methylated  
210 positions (DMP) (FDR < 0.01) comparing rs10423769\_A to rs10423769\_G haplotypes. Further  
211 analysis indicated that differences in methylation on those positions occurred due to base  
212 changes in the haplotype sequences between rs10423769\_A to rs10423769\_G haplotypes, with  
213 gain or loss of CpG sites (Figure 7).



214  
215 **Figure 7.** Allele-specific differential methylation analysis in the rs10423769\_A allele 21 kb minimum shared haplotype and surrounding  
216 region using 5 brain samples heterozygous for rs10423769. The dotted line indicates FDR < 0.01. "Methylation diff" refers to the  
217 difference in mean methylation levels between the rs10423769\_A and rs10423769\_G haplotypes. "Methylation diff" is shown for DMP  
218 with FDR < 0.01.

219  
220 **Discussion**

221 Herein we report the initial efforts to characterize the protective locus tagged by the A  
222 allele of rs10423769 which reduces the AD risk effect in AFR ancestry *APOE* $\epsilon$ 4 homozygotes by

223 approximately 75%. Understanding the mechanisms involved in the protective effect is  
224 challenging, since the variant is located 2 Mb away from *APOE*, in a large area of SD containing  
225 a *PSG* gene cluster composed of 10 genes (*PSG1-9*, *PSG11*). Given the SD in the region, one  
226 of the first questions to answer was whether the locus was unique or duplicated. We demonstrate  
227 that it is a unique feature lying in a large area of segmental duplications. We confirmed that the  
228 minimum shared haplotype is from AFR origin and is found in all AFR populations represented in  
229 1000 Genomes and admixed AFR populations, but not in Mexican ancestry, Peruvian, East Asian,  
230 South Asian and European populations. The presence of the haplotype in both Western and  
231 Eastern African populations suggests it is likely old in its AFR origin.

232 The haplotype of ~21kb shared by all rs10423769\_A carriers and the extended haplotype  
233 of another 11 kb in high LD with rs10423769\_A ( $r^2 = 0.75$ ) overlap with the lncRNA (*PSG11-AS1/*  
234 *ENSG00000282943*) (Supplementary figure 1). Overall, this lncRNA is expressed in all tissues at  
235 very low levels in the cerebral cortex according to The Genotype-Tissue Expression (GTEx)  
236 Project Release V8 ([Web resources](#)), with cerebellum, cerebellar hemisphere, and cultured  
237 fibroblasts having higher levels of expression.<sup>21</sup> In contrast, the *PSG* genes belong to family of  
238 glycoproteins that are primarily expressed in the human placenta.<sup>4,5</sup> Interestingly, data from the  
239 Allen Institute for Brain Science ([Web resources](#)) suggest that *APOE* has its highest overall  
240 expression just before and after birth. More studies will be needed to elucidate any potential  
241 involvement of the *PSG* genes or lncRNA directly in the protective effect on *APOE* $\epsilon$ 4.

242 The *PSG* locus was previously reported to have a higher frequency of copy number  
243 variations, deletions and duplications, compared to the genome average, with differences in  
244 frequency and distinct breakpoints between AFR and non-AFR haplotypes.<sup>4,22</sup> However, given  
245 the duplication pattern in this region, the reliability of such reports is uncertain. Thus, we used  
246 LRWGS around the SD to characterize the region and the protective and non-protective  
247 haplotypes. We did not see obvious evidence of the SV patterns previously reported. This may

248 be because of the technological limitations of these previous reports that cannot account for  
249 potential changes in segmental duplication patterns between individuals that may be reported as  
250 SVs. Gaining a better understanding of the genomic structure of this locus is critical since it is  
251 possible that differences in SVs or pattern of SDs between the protective and the risk haplotypes  
252 could influence chromatin interactions or other regulatory mechanisms in the area. In fact, it has  
253 been shown that chromatin reorganization happening during cellular aging leads to the re-  
254 expression of *PSG* genes,<sup>23</sup> suggesting a possibility of differences in SV affecting *PSG* gene  
255 expression. While the depth of reads allowed us to validate the structure of the protective  
256 haplotype, it was not enough to allow assembly of the entire 0.55 Mb SD region. This will require  
257 a much higher read depth, perhaps as high as 100x.

258         Several neurodegenerative diseases have been associated with VNTRs<sup>24</sup> in general and  
259 AD specifically. For example, increased length of a 25 bp repeat unit located in intron 18 of *ABCA7*  
260 was associated with increased AD risk.<sup>25</sup> Interestingly, the protective haplotype was associated  
261 with expanded VNTR alleles which are enriched for a 29 bp motif with multiple MEF2 binding  
262 motifs. These types of clusters and VNTRs can be found in many areas of the genome, but what  
263 is compelling here is the significantly larger VNTR associated with the protective haplotype vs.  
264 the non-protective haplotype. The MEF2 family of TF have an important role during both  
265 development and adulthood, participating in neuronal development, synaptic plasticity, cognitive  
266 reserve and neurodegenerative diseases, by controlling the expression of several genes and  
267 miRNAs<sup>26</sup>. The expression of all MEF2 isoforms is high in the brain, with the expression of MEF2A  
268 and MEF2D increasing with neuronal differentiation and maturation, whereas the expression of  
269 MEF2C remains relatively stable throughout.<sup>27</sup> Barker et al. (2022) found that MEF2  
270 transcriptional network demonstrated the strongest association with predictive good cognition  
271 towards the end of life. Overexpression of *MEF2A/C* in a mouse model of tauopathy had positive  
272 effects on cognitive flexibility.<sup>28</sup> However, other authors suggest MEF2 has a negative effect on

273 memory function.<sup>29</sup> Thus, depending on the interaction with other co-factors, such as chromatin-  
274 modifying enzymes or polymerase complex, and the cell type, MEF2s can either activate or  
275 suppress gene expression<sup>27</sup>. It was reported that a MEF2A variant (p.Pro279Leu), which  
276 decreases MEF2A's function in transcriptional activity, was significantly enriched in LOAD  
277 patients.<sup>30</sup> In addition, elevated methylation at an enhancer region of *MEF2A* that reduced *MEF2A*  
278 expression has been reported in AD,<sup>31</sup> further linking MEF2 decreased activity with AD. Further  
279 studies are needed to investigate if and how this VNTR may contribute to lowering *APOE*ε4 risk.

280 Differences in methylation status between AD cases and controls have been noted,  
281 including in the *APOE* region.<sup>32–34</sup> We identified several DMP in the protective haplotype, 2 Mb  
282 away from *APOE*. Long-range effects of methylation as far as 10 Mb from promoter regions have  
283 been documented to play a role in regulation of gene expression.<sup>35</sup> Therefore, further follow-up  
284 of these DMPs is needed to determine the role of these alterations on *APOE* expression  
285 specifically or other genes in the region, and on AD risk in general.

286 One important question to be addressed in the future is whether the protective association  
287 of rs10423769\_A with *APOE*ε4 involves lowering of *APOE*ε4 expression. Single nuclei RNA-  
288 sequencing data from our group suggests that the expression of *APOE* is much lower in one  
289 individual who is an *APOE* ε4/ε4 carrier and homozygote for rs10423769\_A when compared to  
290 rs10423769\_G carriers.<sup>9</sup> Efforts are underway to identify brain material carrying both the  
291 rs10423769\_A allele and *APOE*ε4, but the low availability of tissue from the African ancestry  
292 population makes this more challenging.

293 Overall, while dozens of risk variants for AD have been described over the last decade,  
294 protective variants for AD have received less attention. Through evolution, protective  
295 mechanisms, usually with minimal side effects, have been established naturally. Increasing the  
296 number of studies on these protective variants to understand their processes is essential for the  
297 advancement of therapeutics in AD. In addition, our study illustrates the importance of including

298 diverse populations in genetics studies to ensure broad representation and open opportunities to  
299 uncover and understand Alzheimer disease and biological mechanisms from a wider perspective.

### 300 **Data and Code Availability**

301 Short read WGS from the ADSP is available via NIAGADS (ADSP R4: ng00067.v10) ([Web](#)  
302 [resources](#)). Long read sequencing is available upon request from the corresponding author. No  
303 custom code was created for this manuscript. All data processing was performed using publicly  
304 available software as referred to in the Methods.

### 305 **Declaration of interests**

306 The authors declare no competing interests.

### 307 **Acknowledgments**

308 This research was supported by the National Institute on Aging through the following grant  
309 numbers: U01AG072579, RF1AG059018, R01AG070864, R01AG072547, U01AG066767,  
310 P30AG066511, and U01AG052410. Additional funding was received by a Zenith Award  
311 (Alzheimer's Association, J.M.V), the BrightFocus foundation (A2018425S, J.M.V) and  
312 Alzheimer's Association Research Fellowship to Promote Diversity (AARFD-24-1309441, L.B.N.).  
313 We are grateful to the many participants, researchers, and staff who contributed significantly to  
314 this study.

### 315 **Web resources**

316 Alzheimer's Disease Sequencing Project Release 4, <https://adsp.niagads.org/>  
317 Plink v1.90, [www.cog-genomics.org/plink/1.9/](http://www.cog-genomics.org/plink/1.9/)  
318 LDhap and LDlink, <https://ldlink.nih.gov/>  
319 Integrative Genome Viewer (IGV), <http://software.broadinstitute.org/software/igv/>  
320 TREAT (Tandem REpeat Annotation Toolkit), <https://github.com/holstegelab/treat/>  
321 MEME Suite, <https://meme-suite.org/meme/tools/meme/>

- 322 FIMO, <https://meme-suite.org/meme/tools/fimo/>
- 323 Modkit, <https://github.com/nanoporetech/modkit/>
- 324 Tandem repeat annotation, <https://github.com/PacificBiosciences/pbsv/tree/master/annotations/>
- 325 BrainSpan Atlas of the Developing Human Brain (Allen Institute for Brain Science),
- 326 <https://www.brainspan.org/rnaseq/search/index.html>
- 327 Genotype-Tissue Expression (GTEx), <https://www.gtexportal.org/>



## References

1. Rajabli, F., Feliciano, B.E., Celis, K., Hamilton-Nelson, K.L., Whitehead, P.L., Adams, L.D., Bussies, P.L., Manrique, C.P., Rodriguez, A., Rodriguez, V., et al. (2018). Ancestral origin of ApoE  $\epsilon$ 4 Alzheimer disease risk in Puerto Rican and African American populations. *PLoS Genet* *14*, 1–13. <https://doi.org/10.1371/journal.pgen.1007791>.
2. Blue, E.E., Horimoto, A.R.V.R., Mukherjee, S., Wijsman, E.M., and Thornton, T.A. (2019). Local ancestry at APOE modifies Alzheimer's disease risk in Caribbean Hispanics. *Alzheimer's & Dementia* *15*, 1524–1532. <https://doi.org/10.1016/j.jalz.2019.07.016>.
3. Rajabli, F., Beecham, G.W., Hendrie, H.C., Baiyewu, O., Ogunniyi, A., Gao, S., Kushch, N.A., Lipkin-Vasquez, M., Hamilton-Nelson, K.L., Young, J.I., et al. (2022). A locus at 19q13.31 significantly reduces the ApoE  $\epsilon$ 4 risk for Alzheimer's Disease in African Ancestry. *PLoS Genet* *18*, e1009977. <https://doi.org/10.1371/journal.pgen.1009977>.
4. Chang, C.L., Semyonov, J., Cheng, P.J., Huang, S.Y., Park, J. II, Tsai, H.-J., Lin, C.-Y., Grützner, F., Soong, Y.K., Cai, J.J., et al. (2013). Widespread Divergence of the CEACAM/PSG Genes in Vertebrates and Humans Suggests Sensitivity to Selection. *PLoS One* *8*, e61701. <https://doi.org/10.1371/journal.pone.0061701>.
5. Moore, T., and Dveksler, G.S. (2014). Pregnancy-specific glycoproteins: complex gene families regulating maternal-fetal interactions. *Int J Dev Biol* *58*, 273–280. <https://doi.org/10.1387/ijdb.130329gd>.
6. Vollger, M.R., Dishuck, P.C., Harvey, W.T., DeWitt, W.S., Guitart, X., Goldberg, M.E., Rozanski, A.N., Lucas, J., Asri, M., Abel, H.J., et al. (2023). Increased mutation and gene conversion within human segmental duplications. *Nature* *2023* 617:7960 617, 325–334. <https://doi.org/10.1038/s41586-023-05895-y>.
7. Bailey, J.A., Gu, Z., Clark, R.A., Reinert, K., Samonte, R. V., Schwartz, S., Adams, M.D., Myers, E.W., Li, P.W., and Eichler, E.E. (2002). Recent segmental duplications in the human genome. *Science* (1979) *297*, 1003–1007. <https://doi.org/10.1126/science.1072047>.
8. Sharp, A.J., Locke, D.P., McGrath, S.D., Cheng, Z., Bailey, J.A., Vallente, R.U., Pertz, L.M., Clark, R.A., Schwartz, S., Seagraves, R., et al. (2005). Segmental duplications and copy-number variation in the human genome. *Am J Hum Genet* *77*, 78–88. <https://doi.org/10.1086/431652>.
9. Celis, K., Moreno, M.D.M.M., Rajabli, F., Whitehead, P., Hamilton-Nelson, K., Dykxhoorn, D.M., Nuytemans, K., Wang, L., Flanagan, M., Weintraub, S., et al. (2023). Ancestry-related differences in chromatin accessibility and gene expression of APOE  $\epsilon$ 4 are associated with Alzheimer's disease risk. *Alzheimer's & Dementia*. <https://doi.org/10.1002/ALZ.13075>.
10. Griswold, A.J., Celis, K., Bussies, P.L., Rajabli, F., Whitehead, P.L., Hamilton-Nelson, K.L., Beecham, G.W., Dykxhoorn, D.M., Nuytemans, K., Wang, L., et al. (2021). Increased APOE  $\epsilon$ 4 expression is associated with the difference in Alzheimer's disease risk from diverse ancestral backgrounds. *Alzheimer's and Dementia* *17*, 1179–1188. <https://doi.org/10.1002/alz.12287>.
11. Auton, A., Abecasis, G.R., Altshuler, D.M., Durbin, R.M., Bentley, D.R., Chakravarti, A., Clark, A.G., Donnelly, P., Eichler, E.E., Flicek, P., et al. (2015). A global reference for human genetic variation. *Nature* *526*, 68–74. <https://doi.org/10.1038/nature15393>.
12. Wang, N., Akey, J.M., Zhang, K., Chakraborty, R., and Jin, L. (2002). Distribution of recombination crossovers and the origin of haplotype blocks: The interplay of population history, recombination, and mutation. *Am J Hum Genet* *71*, 1227–1234. <https://doi.org/10.1086/344398>.
13. Purcell, S., Neale, B., Todd-Brown, K., Thomas, L., Ferreira, M.A.R., Bender, D., Maller, J., Sklar, P., De Bakker, P.I.W., Daly, M.J., et al. (2007). PLINK: A tool set for whole-genome association and population-based linkage analyses. *Am J Hum Genet* *81*, 559–575. <https://doi.org/10.1086/519795>.
14. Machiela, M.J., and Chanock, S.J. (2015). LDlink: A web-based application for exploring population-specific haplotype structure and linking correlated alleles of possible functional variants. *Bioinformatics* *31*, 3555–3557. <https://doi.org/10.1093/bioinformatics/btv402>.
15. Tesi, N., Salazar, A., Zhang, Y., van der Lee, S., Hulsman, M., Knoop, L., Wijesekera, S., Krizova, J., Schneider, A.-F., Pennings, M., et al. (2024). Characterising tandem repeat complexities across long-read sequencing platforms with TREAT and otter. *bioRxiv*, 2024.03.15.585288. <https://doi.org/10.1101/2024.03.15.585288>.

16. Bailey, T.L., Johnson, J., Grant, C.E., and Noble, W.S. (2015). The MEME Suite. *Nucleic Acids Res* **43**, W39–W49. <https://doi.org/10.1093/nar/gkv416>.
17. Grant, C.E., Bailey, T.L., and Noble, W.S. (2011). FIMO: scanning for occurrences of a given motif. *Bioinformatics* **27**, 1017–1018. <https://doi.org/10.1093/bioinformatics/btr064>.
18. Castro-Mondragon, J.A., Riudavets-Puig, R., Rauluseviciute, I., Berhanu Lemma, R., Turchi, L., Blanc-Mathieu, R., Lucas, J., Boddie, P., Khan, A., Manosalva Pérez, N., et al. (2022). JASPAR 2022: the 9th release of the open-access database of transcription factor binding profiles. *Nucleic Acids Res* **50**, D165–D173. <https://doi.org/10.1093/nar/gkab1113>.
19. Edge, P., and Bansal, V. (2019). Longshot enables accurate variant calling in diploid genomes from single-molecule long read sequencing. *Nat Commun* **10**. <https://doi.org/10.1038/s41467-019-12493-y>.
20. Akbari, V., Garant, J.M., O’Neill, K., Pandoh, P., Moore, R., Marra, M.A., Hirst, M., and Jones, S.J.M. (2021). Megabase-scale methylation phasing using nanopore long reads and NanoMethPhase. *Genome Biol* **22**, 1–21. <https://doi.org/10.1186/s13059-021-02283-5>.
21. Carithers, L.J., Ardlie, K., Barcus, M., Branton, P.A., Britton, A., Buia, S.A., Compton, C.C., DeLuca, D.S., Peter-Demchok, J., Gelfand, E.T., et al. (2015). A Novel Approach to High-Quality Postmortem Tissue Procurement: The GTEx Project. *Biopreserv Biobank* **13**, 311–319. <https://doi.org/10.1089/bio.2015.0032>.
22. Sudmant, P.H., Rausch, T., Gardner, E.J., Handsaker, R.E., Abyzov, A., Huddleston, J., Zhang, Y., Ye, K., Jun, G., Fritz, M.H.Y., et al. (2015). An integrated map of structural variation in 2,504 human genomes. *Nature* **526**, 75–81. <https://doi.org/10.1038/nature15394>.
23. Liu, Z., Ji, Q., Ren, J., Yan, P., Wu, Z., Wang, S., Sun, L., Wang, Z., Li, J., Sun, G., et al. (2022). Large-scale chromatin reorganization reactivates placenta-specific genes that drive cellular aging. *Dev Cell* **57**, 1347–1368.e12. <https://doi.org/10.1016/j.devcel.2022.05.004>.
24. Wang, H., Wang, L.-S., Schellenberg, G., and Lee, W.-P. (2023). The role of structural variations in Alzheimer’s disease and other neurodegenerative diseases. *Front Aging Neurosci* **14**. <https://doi.org/10.3389/fnagi.2022.1073905>.
25. De Roeck, A., Duchateau, L., Van Dongen, J., Cacace, R., Bjerke, M., Van den Bossche, T., Cras, P., Vandenberghe, R., De Deyn, P.P., Engelborghs, S., et al. (2018). An intronic VNTR affects splicing of ABCA7 and increases risk of Alzheimer’s disease. *Acta Neuropathol* **135**, 827–837. <https://doi.org/10.1007/s00401-018-1841-z>.
26. Lisek, M., Przybyszewski, O., Zylinska, L., Guo, F., and Boczek, T. (2023). The Role of MEF2 Transcription Factor Family in Neuronal Survival and Degeneration. *Int J Mol Sci* **24**. <https://doi.org/10.3390/ijms24043120>.
27. Assali, A., Harrington, A.J., and Cowan, C.W. (2019). Emerging roles for MEF2 in brain development and mental disorders. *Curr Opin Neurobiol* **59**, 49–58. <https://doi.org/10.1016/j.conb.2019.04.008>.
28. Barker, S.J., Raju, R.M., Wang, J., Davila-velderrain, J., Abdurrob, F., Milman, N.E.P., Abdelaal, K., Ashley, L., Yu, L., Bennett, D.A., et al. (2022). MEF2s are key regulators of cognitive function and confer resilience to neurodegeneration. *13*. <https://doi.org/10.1126/scitranslmed.abd7695>. MEF2s.
29. Rashid, A.J., Cole, C.J., and Josselyn, S.A. (2014). Emerging roles for MEF2 transcription factors in memory. *Genes Brain Behav* **13**, 118–125. <https://doi.org/10.1111/gbb.12058>.
30. González, P., Álvarez, V., Menéndez, M., Lahoz, C.H., Martínez, C., Corao, A.I., Calatayud, M.T., Peña, J., García-Castro, M., and Coto, E. (2007). Myocyte enhancing factor-2A in Alzheimer’s disease: Genetic analysis and association with MEF2A-polymorphisms. *Neurosci Lett* **411**, 47–51. <https://doi.org/10.1016/j.neulet.2006.09.055>.
31. Li, H., Wang, F., Guo, X., and Jiang, Y. (2021). Decreased MEF2A Expression Regulated by Its Enhancer Methylation Inhibits Autophagy and May Play an Important Role in the Progression of Alzheimer’s Disease. *Front Neurosci* **15**, 1–15. <https://doi.org/10.3389/fnins.2021.682247>.
32. Shireby, G., Dempster, E.L., Policicchio, S., Smith, R.G., Pishva, E., Chioza, B., Davies, J.P., Burrage, J., Lunnon, K., Seiler Vellame, D., et al. (2022). DNA methylation signatures of Alzheimer’s disease neuropathology in the cortex are primarily driven by variation in non-neuronal cell-types. *Nat Commun* **13**, 1–14. <https://doi.org/10.1038/s41467-022-33394-7>.
33. Foraker, J., Millard, S.P., Leong, L., Thomson, Z., Chen, S., Keene, C.D., Bekris, L.M., Yu, C.E., and Fischer, A. (2015). The APOE Gene is Differentially Methylated in Alzheimer’s Disease. *Journal of Alzheimer’s Disease* **48**, 745–755. <https://doi.org/10.3233/JAD-143060>.

34. Liu, J., Zhao, W., Ware, E.B., Turner, S.T., Mosley, T.H., and Smith, J.A. (2018). DNA methylation in the APOE genomic region is associated with cognitive function in African Americans. *BMC Med Genomics* *11*, 1–13. <https://doi.org/10.1186/s12920-018-0363-9>.
35. Kim, S., Park, H.J., Cui, X., and Zhi, D. (2020). Collective effects of long-range DNA methylations predict gene expressions and estimate phenotypes in cancer. *Sci Rep* *10*, 1–12. <https://doi.org/10.1038/s41598-020-60845-2>.